

# Electrical conductivity in graphene with point defects

Yuriy V. Skrypnyk<sup>1</sup> and Vadim M. Loktev<sup>2</sup>

<sup>1</sup>*G. V. Kurdyumov Institute of Metal Physics,*

*National Academy of Sciences of Ukraine Vernadsky Ave. 36, Kyiv 03680, Ukraine*

<sup>2</sup>*Bogolyubov Institute for Theoretical Physics,*

*National Academy of Sciences of Ukraine Metrolohichna Str. 14-b, Kyiv 03680, Ukraine*

## Abstract

The electrical conductivity of graphene containing point defects is studied within the binary alloy model in its dependence on the Fermi level position at the zero temperature. It is found that the minimal conductivity value does not have a universal character and corresponds to the impurity resonance energy rather than to the Dirac point position in the spectrum. The substantial asymmetry of the resulting dependence of the conductivity on the gate voltage magnitude is attributed as well to the very shift of the conductivity minimum to the resonance state energy.

PACS numbers: 71.23.-k, 71.55.-i, 81.05.ue

## I. INTRODUCTION

Graphene, a thermodynamically stable graphite monolayer, which has been mechanically exfoliated for the first time only a few years ago,<sup>1-3</sup> is gaining considerable scientific attention. This new material looks promising enough for a number of important practical applications, some of which have been long hoped for. While experimenters are targeted at engineering graphene based devices in the not so distant future, graphene attracts theoreticians as the first existing in the free state physical system, which can be named two-dimensional (2D) without any reservations. Undoubtedly, so far unique electronic properties of graphene were the most challenging issue. These properties directly come up from the honeycomb lattice with its two-atomic structure, inherent in a single atomic layer of graphite. The lattice structure leads to the Dirac dispersion of charge carriers, which makes up the core of studies devoted to graphene.

Transport properties of this material are, sure enough, of primary importance for graphene-based electronics. In real crystals, transport properties essentially depend on non-ideality of the system and on interaction of carriers with other excitations. Below we are going to focus on imperfections of graphene, and, in particular, on point defects in it. This allows to rise a question on the spectrum of delocalized carriers, on its dependence on the amount of defects, and, eventually, on such a remarkable quantity as the minimal value of the conductivity.

Initially, two main features of the graphene conductivity were singled out. First of all, the conductivity of graphene devices never dropped below a certain value. Since this minimal value seemed not to vary between different experimental samples, the origin of the universal behavior of the minimal conductivity value has been extensively searched for. These efforts shaped the famous *minimum conductivity* puzzle. The linear dependence of the conductivity on the gate voltage made up the second feature. However, the minimal conductivity value has been found soon to be strongly sample dependent,<sup>4</sup> and the effect of minimum conductivity has been attributed to graphene's imperfections. In view of mentioned features of the graphene conductivity, a qualitative difference between charged impurities and point defects has been established.<sup>5</sup> While it has been demonstrated that charged impurities are able to yield the required linear dependence of conductivity on the gate voltage, point defects were shown to produce the sub-linear conductivity behavior, and, consequently, ruled out as

the conductivity limiting factor. The concept of charged impurities as a main source of the scattering of charge carriers in graphene has been thoroughly developed,<sup>6–8</sup> and convincingly compared to the experimental data on graphene with deposited potassium atoms on its surface.<sup>9,10</sup> At that, just a constant contribution to the conductivity were ascribed to point defects when fitting the experimental data.

Even though the concept of charged impurities looks sounding, experiments on graphene in ethanol environment seriously question the dominant role of the Coulomb scatterers.<sup>11</sup> In addition, the conductivity asymmetry evident in measurements of graphene with deposited potassium atoms has not received the proper explanation yet.<sup>9,10</sup> While a moderate asymmetry can be attributed to the disbalance of positively and negatively charged impurities,<sup>12</sup> the marked asymmetry of conductivity dependence on the gate voltage in graphene doped by transition metals manifests the response that is different from the one, which is expected from the charged impurity centers.<sup>13</sup> The clearly sub-linear character of conductivity curves corresponding to graphene samples heavily doped by transition metals or lightly doped by the potassium atoms only strengthen the overall impression that we are dealing with the interplay of different types of disorder, and that each one of them should receive a comprehensive treatment in an effort to grasp the conductivity properties in graphene. As an example, an interplay between charged impurities and point defects, which involves different reaction of these two impurity types to screening effects, can be employed to solve the dilemma of slightly varying minimal conductivity value for graphene placed into a dielectric environment.<sup>14</sup>

It must be stressed that in the mentioned experiments targeted at finding the main scattering channel for carriers in graphene, different adatoms were deposited on the surface of samples, which otherwise were considered as pristine. In fact, here we are dealing with two different issues again. One of them is determining what actually limits the conductivity of graphene samples obtained by a certain technique, and another one is analyzing the effect of intentionally added impurities on the conductivity features. The latter is closely related to the current tendency to functionalize graphene by substitutionals, adatoms, or chemically active groups. Regarding the conducting properties, such an adjustment of graphene can proceed up to a possibility of the metal–insulator transition, which has been successfully observed in graphene doped by hydrogen atoms recently.<sup>15</sup> Similarly, graphene demonstrated insulating behavior after irradiation by Ne ions, which is expected to produce short-range

defects.<sup>16</sup>

In view of that, before any complex models of impurity centers are constructed, the simple ones should be properly examined in their characteristic aspects. And the basic model of the point defect is definitely among them, since it allows for a Mott transition in impure graphene.<sup>17</sup>

Below we are returning to the common in semiconductor physics model of a binary alloy intending to examine what features of the graphene conductivity it is capable to reproduce. Such short-range impurities violate the electron-hole symmetry of the system and are naturally providing for the conductivity asymmetry. This impurity model has been studied either in a weak scattering limit, or in the unitary limit. We are going to show that this model does exhibit some worthwhile features in-between these two extremes. In particular, we demonstrate that the effective conductivity minimum, in contrast to former studies, corresponds not to the Dirac point of the spectrum, but to the energy of a single impurity resonance, where the impurity scattering is the strongest.

## II. MODEL DISORDERED SYSTEM

The host Hamiltonian for electrons in graphene is taken in the tight binding approximation with hopping restricted to the nearest neighbors,

$$\mathbf{H}_0 = t \sum_{\langle \mathbf{n}\alpha, \mathbf{m}\beta \rangle} c_{\mathbf{n}\alpha}^\dagger c_{\mathbf{m}\beta}, \quad (1)$$

where  $t \approx 2.7\text{eV}$  is the hopping parameter for the nearest neighbors,<sup>18</sup>  $\mathbf{n}$  and  $\mathbf{m}$  run over lattice cells,  $\alpha$  and  $\beta$  enumerate two sublattices of the honeycomb atomic arrangement,  $c_{\mathbf{n}\alpha}^\dagger$  and  $c_{\mathbf{n}\alpha}$  are the electron creation and annihilation operators at the respective lattice sites. Substitutional impurities are supposed to be distributed evenly and in uncorrelated manner on lattice sites. Presence of an impurity at a given lattice site is assumed to be manifested only through a change in the respective on-site potential of the tight-binding Hamiltonian. This type of impurity perturbation fully corresponds to the conventional model of a binary alloy with a diagonal disorder, which had been extensively used in physics of real crystals, and sometimes is referred to as the Lifshitz (or isotopic) model for historical reasons. The

corresponding Hamiltonian for a disordered graphene has the form,

$$\mathbf{H} = \mathbf{H}_0 + \mathbf{H}_{imp}, \quad \mathbf{H}_{imp} = V_L \sum_{\mathbf{n}, \alpha} \eta_{\mathbf{n}\alpha} c_{\mathbf{n}\alpha}^\dagger c_{\mathbf{n}\alpha}, \quad (2)$$

where  $V_L$  is the deviation of the potential at the impurity site, and variable  $\eta_{\mathbf{n}\alpha}$  is unity with the probability  $c$  or zero with the probability  $(1 - c)$ , which specifies  $c$  as the impurity concentration. The ‘‘per carbon atom’’ concentration  $c$  can be easily converted to the impurity coverage,

$$n_{im} = n_0 c, \quad (3)$$

where

$$n_0 = \frac{4}{\sqrt{3}a^2} \quad (4)$$

is the inverse area per one carbon atom, and  $a = 0.246$  nm is the lattice constant of graphene.

The Green’s function of a disordered system,

$$\mathbf{g} = (E - \mathbf{H})^{-1}, \quad (5)$$

after averaging over different impurity distributions,  $\mathbf{G} = \langle \mathbf{g} \rangle$ , regains the translational invariance and can be expressed by means of the Dyson equation,

$$\mathbf{G} = \mathbf{g} + \mathbf{g} \mathbf{\Sigma} \mathbf{G}, \quad (6)$$

where  $\mathbf{\Sigma}$  is the self-energy, and

$$\mathbf{g}(E) = (E - \mathbf{H}_0)^{-1} \quad (7)$$

is the host Green’s function. When the amount of introduced impurities is moderate, it is possible to implement the modified propagator method.<sup>19</sup> Within this approach, the self-energy is site diagonal and identical on both sublattices,

$$\mathbf{\Sigma} \approx \Sigma(E) \mathbf{I}, \quad \Sigma(E) \equiv \Sigma_{\mathbf{n}\alpha\mathbf{n}\alpha}(E) = \frac{cV_L}{1 - V_L g_{\mathbf{n}\alpha\mathbf{n}\alpha}[E - \Sigma(E)]}, \quad (8)$$

where  $\mathbf{I}$  is the identity matrix. At a small impurity concentration,  $c \ll 1$ , multiple occupancy corrections are not significant. Thus, the method of modified propagator yields results that are practically indistinguishable from the ones produced by the conventional coherent potential approximation.

The calculation of the diagonal element of the host Green's function in the site representation  $g_{\mathbf{n}\alpha\mathbf{n}\alpha}$ , which will be required for the subsequent analytical treatment of the impurity problem, is given in Appendix. From here and on we are choosing the bandwidth parameter  $W$ , see Eq. (A.9), as the energy unit. For the sake of clarity, we will use for the dimensionless energy and the impurity potential following designations:

$$\epsilon = \frac{E}{W}, \quad v = \frac{V_L}{W}, \quad (9)$$

Since only energies small compared to the bandwidth, i.e. those, at which the linear dispersion holds in the host system, are considered, the corresponding approximation to the dimensionless diagonal element of the Green's function can be written as follows,

$$W g_{\mathbf{n}\alpha\mathbf{n}\alpha}(E) \equiv g_0(\epsilon) \approx 2\epsilon \ln |\epsilon| - i\pi |\epsilon|, \quad |\epsilon| \ll 1. \quad (10)$$

It is not difficult to see that the diagonal element of the Green's function (10) looks similar to the properly scaled diagonal element obtained within the model of massless Dirac fermions for the electron spectrum in graphene. Thus, despite the fact, that the intervalley scattering is, for sure, taken into account in Eq. (8) explicitly, the net result for the single-site scattering will not be qualitatively different from the one for the frequently used model of massless Dirac fermions, in which only one Dirac cone is retained. This resemblance follows from the single-site character of the impurity perturbation (see Eq. (2)). At that, the validity of the modified propagator method (8) is limited by the scatterings on impurity clusters,<sup>17,20</sup> which contribution to the self-energy will be monitored in what follows.

### III. RENORMALIZED ENERGY PHASE AND CONDUCTIVITY

In order to make the self-consistency condition (8) more tractable, a regular substitution can be made,

$$\epsilon - \Sigma(\epsilon) = \varkappa \exp(i\varphi), \quad \varkappa > 0, \quad 0 < \varphi < \pi, \quad (11)$$

which singles out the phase of the renormalized energy  $\epsilon - \Sigma(\epsilon)$ . This phase diminishes from  $\pi/2$  to zero inside the conduction band and rise from  $\pi/2$  to  $\pi$  within the valence band when moving away from the Dirac point position. With the help of the obtained above expression (10) for the diagonal element of the Green's function and the substitution (11),

the imaginary part of Eq. (8) can be reduced as follows,

$$cv^2 [2 \ln \varkappa + (2\varphi - \pi) \cot \varphi] + [1 - v\varkappa(2 \ln \varkappa \cos \varphi - (2\varphi - \pi) \sin \varphi)]^2 + [v\varkappa(2 \ln \varkappa \sin \varphi + (2\varphi - \pi) \cos \varphi)]^2 = 0. \quad (12)$$

Provided that the impurity perturbation strength  $v$  and the impurity concentration  $c$  are fixed, this equation establishes a correspondence between the renormalized energy modulus  $\varkappa$  and its phase  $\varphi$ . For those  $\varkappa$  that are exceeding a certain threshold magnitude, which is, indeed, determined by the impurity concentration and the perturbation strength, this equation always has two different solutions with respect to the phase  $\varphi$ . One of them ( $\varphi < \pi/2$ ) belongs to the conduction band, while the other ( $\varphi > \pi/2$ ) lies within the valence band. The literal carrier energy that corresponds to a given renormalized energy is determined by the real part of Eq. (8),

$$\epsilon = \varkappa \cos \varphi + \frac{cv [1 - v\varkappa(2 \ln \varkappa \cos \varphi - (2\varphi - \pi) \sin \varphi)]}{[1 - v\varkappa(2 \ln \varkappa \cos \varphi - (2\varphi - \pi) \sin \varphi)]^2 + [v\varkappa(2 \ln \varkappa \sin \varphi + (2\varphi - \pi) \cos \varphi)]^2}. \quad (13)$$

Taken together, the last two equations, (12) and (13), are making up a set, which implicitly specifies the dependence of the renormalized energy phase  $\varphi$  on the carrier energy  $\epsilon$ .

Since the procedure required to calculate the self-energy is already outlined, it is possible to employ the Kubo expression for the conductivity of a disordered graphene at the zero temperature,<sup>21</sup>

$$\tilde{\sigma}_{cond} = \frac{4e^2}{\pi h} \left\{ 1 + \left[ \frac{\epsilon_F - \text{Re} \Sigma(\epsilon_F)}{-\text{Im} \Sigma(\epsilon_F)} + \frac{-\text{Im} \Sigma(\epsilon_F)}{\epsilon_F - \text{Re} \Sigma(\epsilon_F)} \right] \arctan \left[ \frac{\epsilon_F - \text{Re} \Sigma(\epsilon_F)}{-\text{Im} \Sigma(\epsilon_F)} \right] \right\}, \quad (14)$$

where  $\epsilon_F$  is the Fermi energy. By means of the substitution (11), which was used above to simplify the self-consistency condition for the self-energy (8), the above expression can be significantly reduced,

$$\tilde{\sigma}_{cond} = \left( \frac{e^2}{h} \right) \sigma_{cond}, \quad \sigma_{cond} = \frac{2}{\pi} \left[ 1 + (\cot \varphi_F + \tan \varphi_F) \left( \frac{\pi}{2} - \varphi_F \right) \right], \quad (15)$$

where  $\varphi_F$  is the renormalized energy phase at the Fermi level, and the dimensionless conductivity  $\sigma_{cond}$ , which will be used onwards, is singled out. It should be emphasized that the dimensionless conductivity  $\sigma_{cond}$  depends on the renormalized energy phase  $\varphi$  alone. In the same way, the well-known Ioffe-Regel criterion,<sup>22</sup> which is commonly used to separate

extended states in a disordered system, and the applicability criterion of the modified propagator method can both be expressed through the same renormalized energy phase.<sup>23</sup> It has been shown that with varying the renormalized energy phase the modified propagator approximation validity violation and the indication of the state localization by the Ioffe-Regel criterion are occurring simultaneously for those states, which energies fall inside the host band of a disordered system.<sup>17,23</sup> Certainly, it is not conceptually correct to expect that the Ioffe-Regel criterion can be used to pinpoint precisely the mobility edge position in a disordered system. Similarly, there should be no sharp boundaries between those spectral regions, in which the modified propagator method is applicable, and those ones, in which it is not. Nevertheless, there are strong arguments supporting the estimation that the mobility edge in a disordered system should be located at those energy, at which the renormalized energy phase is close to  $\pi/6$  for the conduction band, and, respectively, to  $5\pi/6$  for the valence band. Thus, in those spectral intervals, inside which states are anticipated to be localized according to the Ioffe-Regel criterion, neither the Kubo formula (15) has any relevance, nor the modified propagator method is reliable. On the contrary, the approach outlined above is consistent in the spectral domains occupied with extended states, where the renormalized energy phase  $\varphi$  is either small (for the conduction band) or close to  $\pi$  (for the valence one).

#### IV. CONDUCTIVITY IN DIFFERENT SCATTERING REGIMES

##### A. Weak scatterers

When the impurity perturbation strength is moderate ( $|v| < 1$ ), it is possible to take an advantage of the renormalized energy phase smallness (or its closeness to  $\pi$ ) and construct a correspondent approximate solution of Eq. (12),

$$\theta \approx \frac{\pi cv^2}{(1 \mp 2v\kappa \ln \kappa)^2 + (\pi v\kappa)^2 + 2cv^2(1 + \ln \kappa)}, \quad \theta \ll 1, \quad (16)$$

where  $\theta$  stands for  $\varphi$  inside the conduction band, and for  $\pi - \varphi$  inside the valence band. The sign in the denominator also switches from a minus to a plus when moving from the conduction band to the valence band. Obviously, the renormalized energy phase is close to  $\pi/2$  in a narrow interval of energies around the shifted Dirac point, and thus the above approximation is not valid inside this region. However, the transition of the renormalized energy phase from small values to values that are close to  $\pi$  is very fast. This transitional



region is, in fact, exponentially narrow and, for certain reasons, should be treated separately, as it will be explained in detail below.

It is not difficult to check that in this scattering regime ( $|v| < 1$ ) the effective shift of states along the energy axis, which is given by the real part of the self-energy  $\text{Re} \Sigma(\epsilon)$ , is nearly constant in the whole domain under consideration ( $|\epsilon| \ll 1$ ). Therefore, as a first approximation, one can take

$$\pm \varkappa \approx \epsilon - cv, \quad (17)$$

where the sign is varying according to the current band as above, so that  $\varkappa$  always remains positive, as it should do. The expression for the conductivity, Eq. (15), can be also simplified utilizing the smallness (or closeness to  $\pi$ ) of the renormalized energy phase,

$$\sigma_{cond} \approx \frac{1}{\theta}, \quad \theta \ll 1, \quad (18)$$

where linear terms and terms of the higher order in  $\theta$  are omitted. All these approximations, Eqs. (16)–(18), can be combined into the final expression for the dimensionless conductivity,

$$\sigma_{cond} \approx \frac{[1 - 2v(\epsilon_F - cv) \ln |\epsilon_F - cv|]^2 + [\pi v(\epsilon_F - cv)]^2}{\pi cv^2} + \frac{2}{\pi} [1 + \ln |\epsilon_F - cv|], \quad (19)$$

which fits well the conductivity, calculated numerically by Eqs. (12),(13), and (15), throughout the whole considered interval of energies ( $|\epsilon| \ll 1$ ).

As follows from (19), the conductivity is gradually diminishing with increasing the Fermi energy  $\epsilon_F$  from the valence band to the conduction band for a negative impurity perturbation ( $v < 0$ ) and vice versa. The conductivity of graphene calculated by Eqs. (12), (13), and (15) without any additional approximations at different concentrations of point defects is plotted against the Fermi energy in Fig. 1 for the case of moderate impurity perturbation ( $|v| < 1$ ). On the whole, the dependence of the conductivity on the Fermi energy is smooth and almost featureless, while being strongly asymmetric against the shifted Dirac point position. The only exception from the monotonic behavior of the conductivity can be observed in a close vicinity of the Dirac point, where the curve manifests a sharp dip, which is barely discernible in the curves corresponding to high impurity concentrations. If to trust the results yielded by the modified propagator method all the way down to the Dirac point, the conductivity at its very tip should drop to  $4/\pi$ . This directly corresponds to the notorious theoretical magnitude of the universal minimum conductivity in the inhomogeneous graphene, which has been widely debated within the so-called “missed  $\pi$ ” discourse. However, the modified

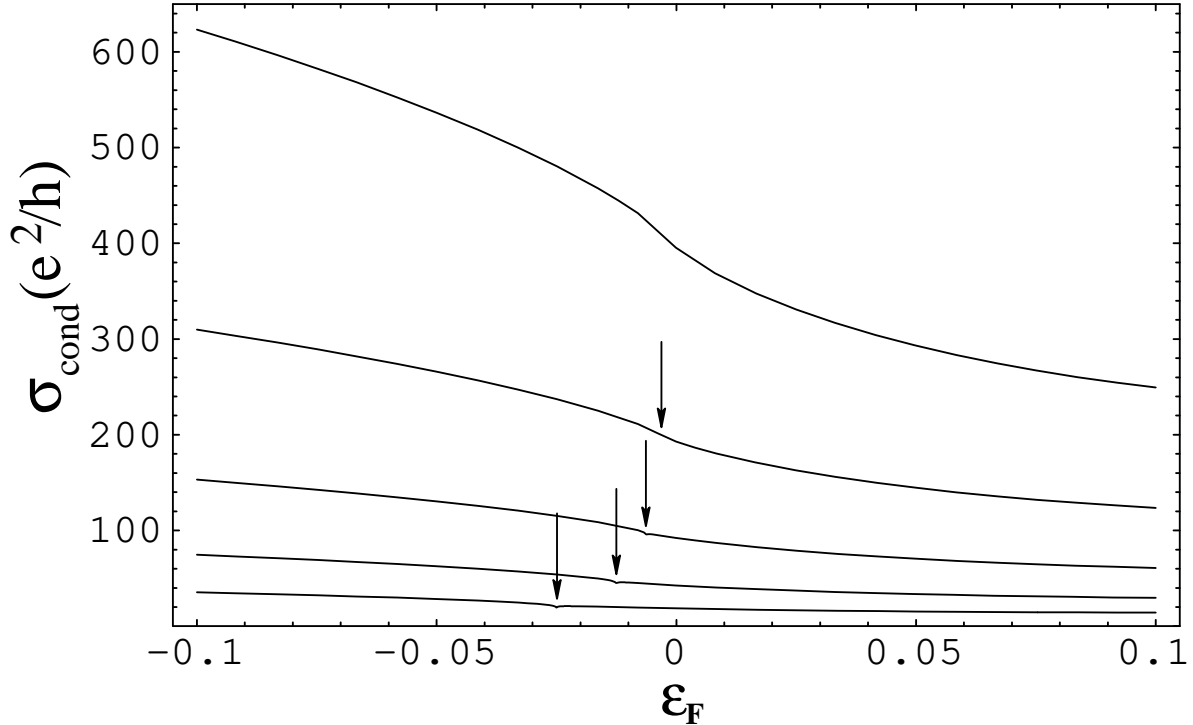


FIG. 1: Conductivity of graphene with point defects *vs* Fermi energy for  $v = -0.5$  and concentrations  $c = 0.1/2^n$ ,  $n = 1 \dots 5$ . Arrows point at positions of narrow dips.

propagator method is not applicable in the Dirac point neighborhood. It can be shown<sup>17,24</sup> that this approximation is not reliable in the interval

$$|\epsilon - cv| \lesssim \exp\left(-\frac{1}{4cv^2} - 1\right). \quad (20)$$

Therefore, as it was outlined in the previous section, the Kubo formula is also ineffective in this interval, and the obtained conductivity magnitude at the Dirac point has no physical meaning. Still, the width of the energy interval, in which the analytical approach fails, is exponentially small compared to the bandwidth. Since the corresponding dip on the conductivity curve is so narrow, it should be averaged out at realistic sample temperature, or by means of any other broadening mechanism.

Consequently, the presence of the sharp dip on the conductivity curve can be neglected, and, probably, should never come out in actual experiments. The asymmetry of the conductivity dependence on the Fermi energy arises from the presence of the severely smeared out impurity resonance, which enhances the impurity scattering. Indeed, the smooth character of the conductivity curve does not resemble the experimentally observed check mark

shape. However, if this check mark shape is caused by another dominating type of impurities, weakly scattering point defects undoubtedly can contribute to the asymmetry of the conductivity curve.

## B. Strong scatterers

In the limit of the strong impurity scattering,  $|v| \gg 1$ , situation is completely different. When the impurity potential is large compared to the bandwidth, a well-defined resonance state is manifested in the electron spectrum.<sup>17</sup> In the limit of a strong impurity potential, the resonance state energy  $\epsilon_r$  is determined by the Lifshitz equation,

$$1 \approx v \operatorname{Re} g_0(\epsilon_r) \approx 2v\epsilon_r \ln |\epsilon_r|, \quad (21)$$

while the resonance state damping is given by

$$\Gamma_r \approx \frac{\pi |\epsilon_r|}{2|1 + \ln |\epsilon_r||}. \quad (22)$$

For the resonance state to be well-defined, the condition

$$\gamma_r \equiv \frac{\Gamma_r}{|\epsilon_r|} \approx \frac{\pi}{2|1 + \ln |\epsilon_r||} \ll 1 \quad (23)$$

must be met. Thus, one should have  $|\ln |\epsilon_r|| \gg 1$ , which corresponds to a strong impurity perturbation and a resonance energy located close to the Dirac point.

The qualitative difference of the strong impurity perturbation case resides not only on the presence of a resonance state in the spectrum, but mainly on the fact that in this case the electron spectrum undergoes a radical rearrangement. That is, with increasing impurity concentration a quasigap filled with localized states opens up around the resonance state energy.<sup>17,20,24</sup> There exists a certain critical concentration of impurities,

$$c_r \sim -\frac{1}{2v^2 \ln(\zeta/|v|)}, \quad \zeta \sim 1, \quad (24)$$

which is determined by the mutual spatial overlap of individual impurity states. When impurity concentration exceeds the critical concentration  $c_r$  of the spectrum rearrangement, the width of the quasigap starts to increase rapidly with increasing impurity concentration as  $\sqrt{-2c/\ln c}$ .<sup>17,20,24</sup> Certainly, neither the modified propagator method nor the Kubo expression for the conductivity will work inside this quasigap. Therefore, we will consider only

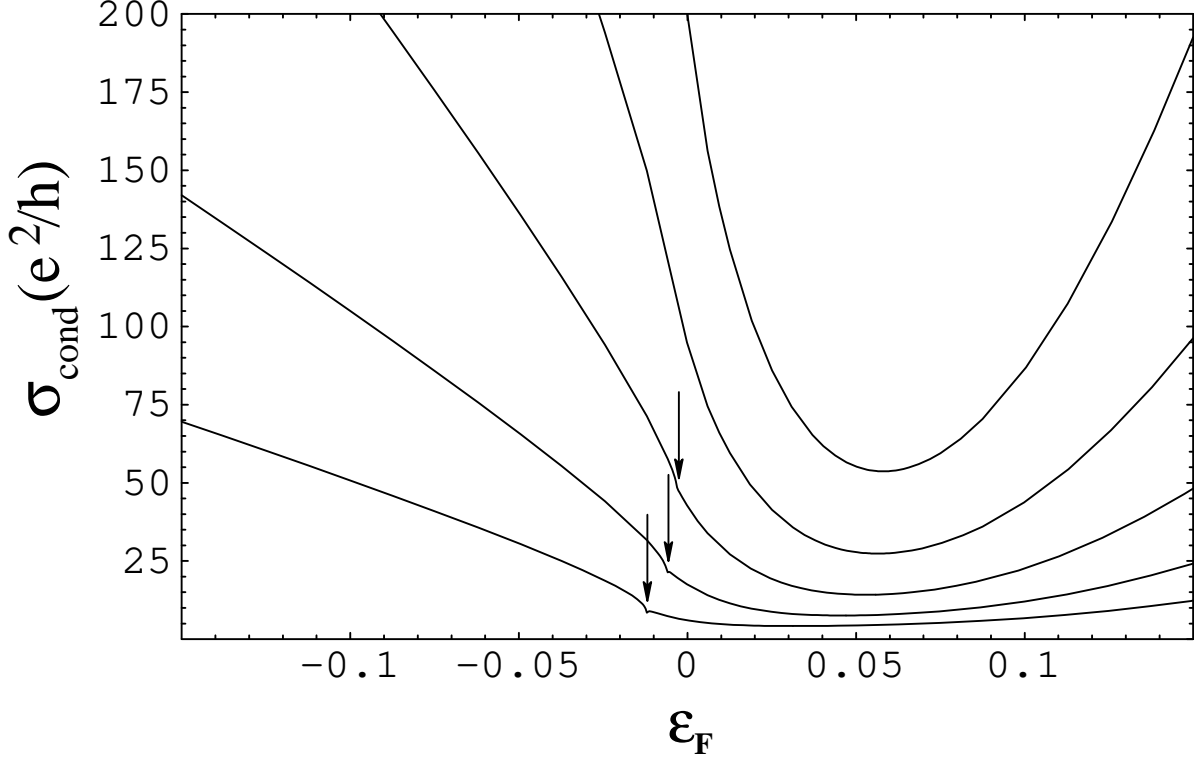


FIG. 2: Conductivity of graphene with point defects *vs* Fermi energy for  $v = -2$  and concentrations  $c = c_r/2^n$ ,  $n = 1 \dots 5$ ,  $c_r \approx 0.012$ . Arrows point at positions of narrow dips.

those impurity concentrations that are less than the critical one ( $c < c_r$ ) in the case of the strong impurity potential. Vacancies are frequently modeled by point defects with infinite impurity potentials  $v$ . Because of this, the critical concentration  $c_r$  for vacancies in graphene is zero. In other words, the spectrum rearrangement is already over for any concentration of vacancies. Therefore, vacancies are out of the scope of the present study.

The conductivity calculated directly by Eqs. (12), (13), and (15) at different concentrations of point defects is shown in Figs. 2 and 3 for a not so excessive ( $v = -2$ ) and for a reasonably strong ( $v = -8$ ) impurity potential, respectively. The Dirac point shift, which occurs along with the impurity concentration increase, is not so pronounced, because  $c_r v \sim 1/v$ . Like in the case of the weak impurity potential, there is a sharp dip in the conductivity curve located at the Dirac point. The hint of this dip can be seen in the figures at concentrations that are approaching the critical one. Nevertheless, the presence of this dip should be neglected by the same arguments as above.

What really distinguishes the strong impurity perturbation case is the presence of the clear

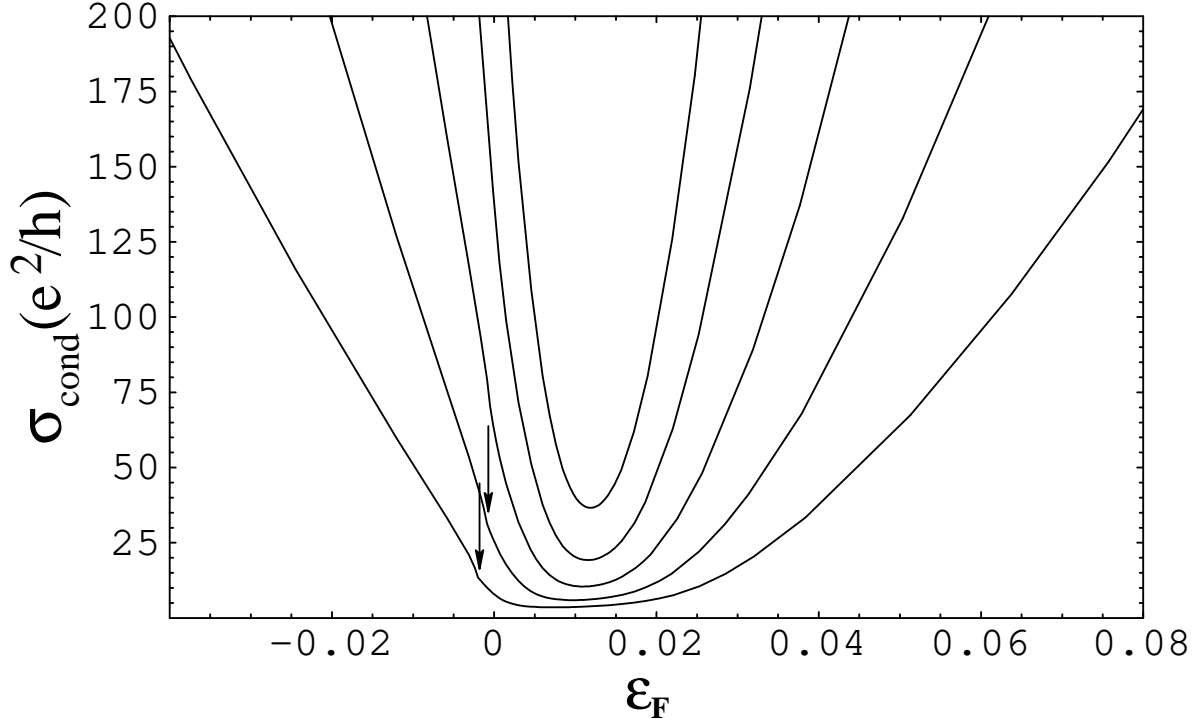


FIG. 3: Conductivity of graphene with point defects *vs* Fermi energy for  $v = -8$  and concentrations  $c = c_r/2^n$ ,  $n = 1 \dots 5$ ,  $c_r \approx 0.0005$ . Arrows point at positions of narrow dips.

minimum on the conductivity curve, which is located at the energy of the impurity resonance state. This is understandable, since the impurity scattering is the strongest around the resonance energy. The width of this minimum corresponds to the resonance state broadening, and, therefore, this minimum is not as sharp as the minimum at the Dirac point. Overall, the conductivity curve acquires a quasi-parabolic form, which is particularly well-pronounced at lower impurity concentrations. In addition, the conductivity curve appears more symmetric for a larger impurity potential.

With increasing the impurity concentration, the concentration broadening of the resonance state also increases. At the impurity concentrations that are close to the critical one, the broadening of the resonance state is as wide as the distance from the resonance energy to the Dirac point. This widening of the resonance broadening area along with the tendency of states toward localization inside it are manifested by the apparent flattening of the conductivity curve around the resonance energy at  $c \sim c_r$ . Outside the domain of the concentration broadening, the approximate expression for the conductivity is even simpler

than before,

$$\sigma_{cond} \approx \frac{[1 - 2v\epsilon_F \ln |\epsilon_F|]^2 + [\pi v\epsilon_F]^2}{\pi c v^2}. \quad (25)$$

It is not difficult to see from Eq. (25) that in the unitary limit,

$$\sigma_{cond}|_{v \rightarrow \infty} \approx \frac{\epsilon_F^2 [(2 \ln |\epsilon_F|)^2 + \pi^2]}{\pi c}, \quad (26)$$

which corresponds to the known result for vacancies in graphene.<sup>25</sup> As was stated above a quasigap around the Dirac point should be present at any impurity concentration in the unitary limit of the impurity perturbation. The approximation (26) is valid only outside of this quasigap.

For the finite impurity perturbation, the expression (25) also can not be used close to the resonance energy. In order to obtain the minimum value of the conductivity, it is required to know the magnitude of the renormalized energy phase at the resonance energy. Its concentration dependence,  $\varphi_r(c)$ , follows from the self-consistency condition (12). The second term in this equation nullifies by the very definition of the resonance energy Eq. (21). The remaining two terms constitute the relation:

$$c = -2\epsilon_r^2(c) \tan \varphi_r(c) \left[ \ln \left| \frac{\epsilon_r(c)}{\cos \varphi_r(c)} \right| \tan \varphi_r(c) + \varphi_r(c) - \frac{\pi}{2} \right]. \quad (27)$$

This expression can be significantly simplified by taking into account that introduced earlier symmetric phase  $\theta$  is small at low impurity concentrations,

$$c \approx \pi \epsilon_r^2(c) \theta_r(c) \left[ 1 + \frac{\theta_r(c)}{\gamma_r} \right], \quad \theta_r(c) \ll 1. \quad (28)$$

Dependence of the resonance energy on the concentration  $\epsilon_r(c)$  is very weak for the strong impurity perturbation and can be neglected. By setting the resonance energy in Eq. (28) to its value for the isolated impurity, this equation can be solved for the renormalized energy phase at the resonance  $\theta_r$ ,

$$\theta_r(c) \approx \frac{\gamma_r}{2} \left( \sqrt{1 + \frac{c}{c^*}} - 1 \right), \quad c^* = \frac{\pi \epsilon_r^2 \gamma_r}{4} \quad (29)$$

The minimum conductivity at the resonance energy is then given by Eq. (18). Indeed, it does not again have the universal character and varies with impurity concentration. The minimum value of conductivity calculated numerically with the help of Eqs. (12), (13) and (15) is plotted against the impurity concentration in Fig. 4 for two different values of the

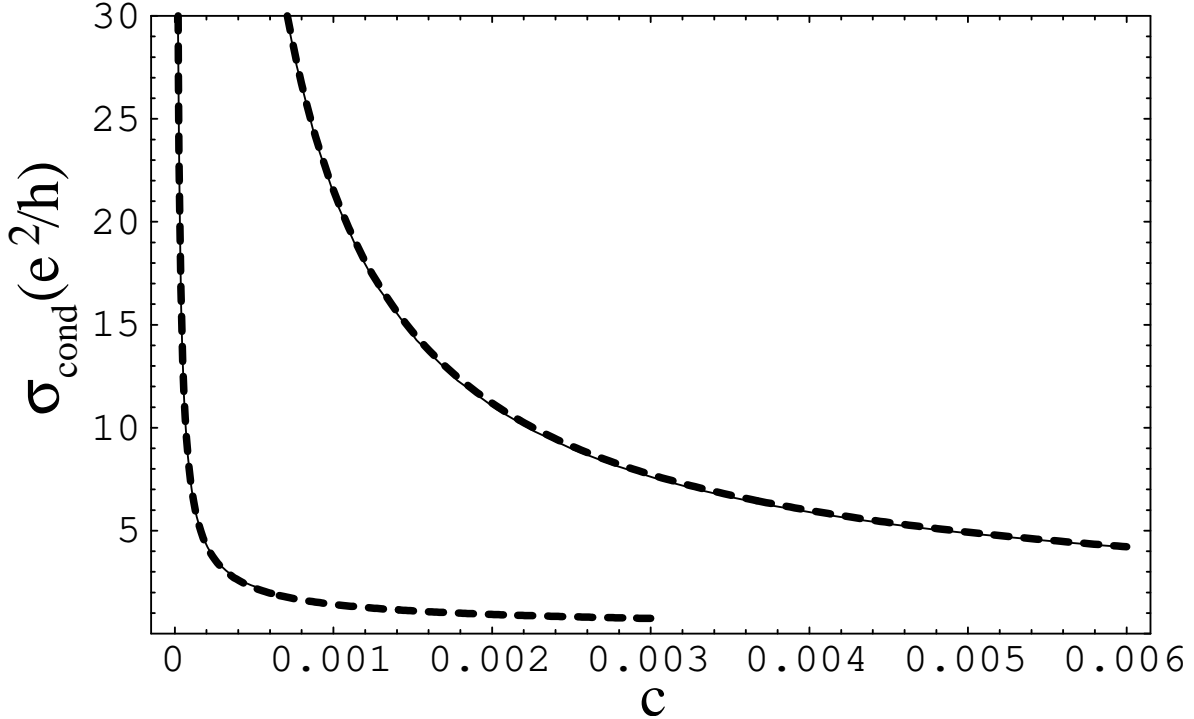


FIG. 4: The minimum conductivity *vs* impurity concentration for  $v = -2$  (upper curve) and for  $v = -8$  (lower curve). Corresponding analytical approximations are given in dashed lines.

impurity potential. Initial fast minimum conductivity drop, which occurs with increasing the impurity concentration, is followed by a considerable flattening of the curve. The manifested saturation-type behavior of the minimum conductivity concentration dynamics qualitatively corresponds to the observed data.<sup>9</sup> According to Eqs. (29) and (18), at small impurity concentrations,  $c \ll c^*$ , the minimum conductivity of graphene with point defects is proportional to  $1/c$ , which is similar to the case of charged impurities.<sup>26</sup> However, at higher impurity concentrations,  $c \gg c^*$ , the minimum conductivity for point defects falls down more slowly, namely as  $1/\sqrt{c}$ . Thus, if both expressions for the minimum conductivity are fitted to each other in the low concentration limit, then the one corresponding to the point defects should yield significantly larger values of the minimum conductivity at  $c \gg c^*$ .

## V. CONDUCTIVITY ASYMMETRY

The conductivity of graphene devices is usually measured against the applied gate voltage. Since the gate voltage controls the carrier density in the graphene sample, these experimental

curves can be simulated by plotting the conductivity as a function of the number of occupied states. Leaving out the irrelevant constant, and taking into account two actual sublattices, the number of occupied states can be written as follows,

$$n(\epsilon_F) = -\frac{2}{\pi} \int_0^{\epsilon_F} \text{Im}(\{\epsilon - \Sigma(\epsilon)\}\{2 \ln[\epsilon - \Sigma(\epsilon)] - i\pi\})d\epsilon. \quad (30)$$

The conductivity of impure graphene, calculated as before by Eqs. (12), (13) and (15), is plotted in Figs. 5 and 6 for both chosen strengths of impurity perturbation against the number of occupied states, which is given by Eq. (30). The number of occupied states is calculated by the numerical integration. The change in the introduced magnitude  $\Delta n(\epsilon_F)$  can be easily related to the respective change in the carrier density  $\Delta n$ ,

$$\Delta n = n_0 \Delta n(\epsilon_F), \quad (31)$$

where  $n_0$  is defined by Eq. (4). In the usual experimental setup, the carrier density depends linearly on the gate voltage  $V^g$ , so  $\Delta n = \chi_V \Delta V^g$ , where  $\chi_V \approx 7.3 \times 10^{10} \text{ cm}^{-2}\text{V}^{-1}$ . Thus, when the gate voltage is varying in the window of  $\pm 100 \text{ V}$ , the value of  $n(\epsilon_F)$  varies by 0.004.

It is visible from Figs. 5 and 6 that the calculated conductivity dependence on the gate voltage is highly asymmetric. Similar asymmetric character of the conductivity curve has been already reported elsewhere for the graphene with point defects.<sup>27</sup> While the expected slightly sublinear behavior of the impure graphene conductivity is readily reproduced, the asymmetry of the curve appears to be a bit on the extreme side. Although such a strong asymmetry is sometimes reported for a graphene with deposited adatoms,<sup>13</sup> its origin for the point defects is to be understood. In order to proceed in this direction, the conductivity can be expanded into a series in the vicinity of its minimum. Since it has been reasoned above that the conductivity reaches its minimum value at the resonance energy  $\epsilon_r$  for the strong impurity perturbation, the expansion is straightforward,

$$\sigma_{cond} \approx \sigma_{cond}^0 + \chi_r (\epsilon_F - \epsilon_r)^2, \quad \chi_r > 0 \quad (32)$$

where  $\sigma_{cond}^0$  is the minimum value of the conductivity, and  $\chi_r$  is some constant.

In the current paper we restrict ourselves for the strong scattering regime to those impurity concentrations that are less than the critical concentration  $c_r$  of the spectrum rearrangement. In this case, the density of states is not considerably distorted by the presence



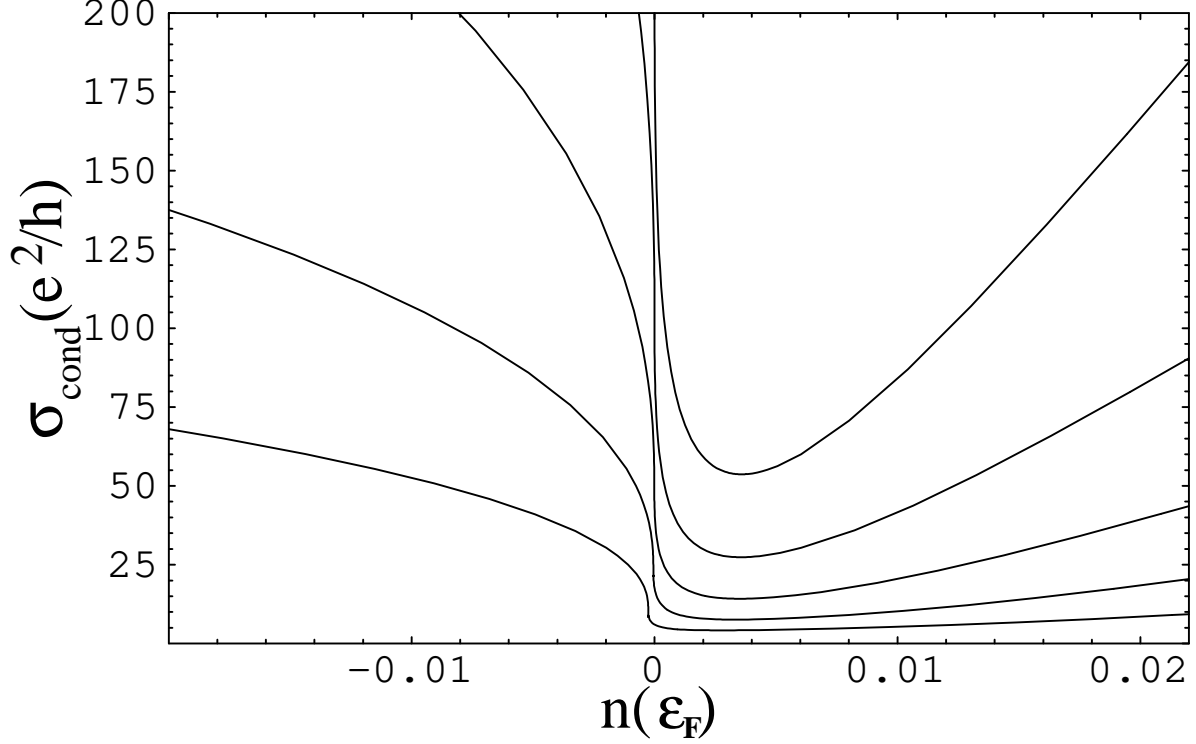


FIG. 5: Conductivity of graphene with point defects *vs* number of carriers for  $v = -2$  and concentrations  $c = c_0/2^n$ ,  $n = 1 \dots 5$ ,  $c_0 \approx 0.012$ .

of defects. Because of the estimative character of this arithmetic, it is quite sufficient to assume that the density of states remains completely unchanged, i.e. identical to the host system, except of the rigid shift of both bands to a new Dirac point  $\epsilon_D$ ,

$$V^g \approx V_D^g + \chi_D(\epsilon_F - \epsilon_D)^2 \text{sgn}(\epsilon_F - \epsilon_D), \quad \chi_D > 0, \quad (33)$$

where  $V_D^g$  is those magnitude of the gate voltage  $V^g$ , at which the Fermi level comes to the Dirac point of the spectrum, and  $\chi_D$  is some constant. This equation can be easily solved for the Fermi energy,

$$\epsilon_F \approx \epsilon_D + \sqrt{\frac{|V^g - V_D^g|}{\chi_D}} \text{sgn}(V^g - V_D^g). \quad (34)$$

Substituting this result to the expansion (32), one can obtain:

$$\sigma_{cond} \approx \sigma_{cond}^0 + \frac{\chi_r}{\chi_D} \left[ \sqrt{|V^g - V_D^g|} \text{sgn}(V^g - V_D^g) - \sqrt{\chi_D}(\epsilon_r - \epsilon_D) \right]^2. \quad (35)$$

It is evident from this relation, that the conductivity asymmetry arise from the shift expressed by the second term in the square brackets. If the conductivity reaches its minimum

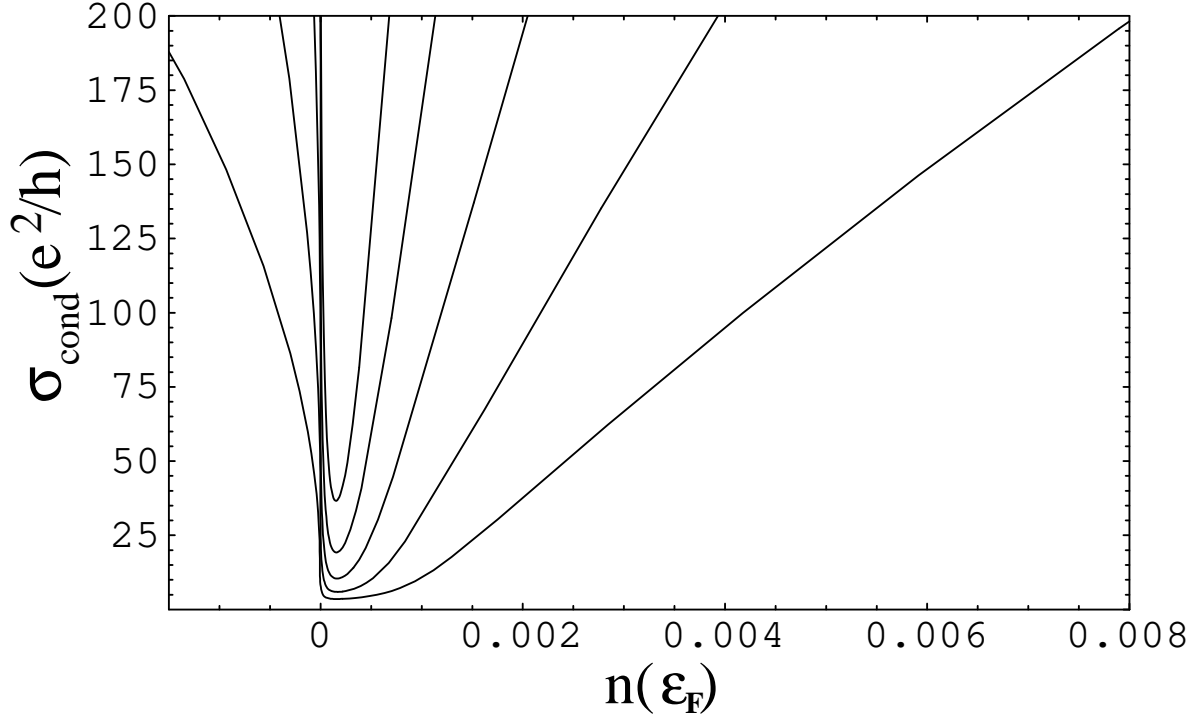


FIG. 6: Conductivity of graphene with point defects *vs* number of carriers for  $v = -8$  and concentrations  $c = c_0/2^n$ ,  $n = 1 \dots 5$ ,  $c_0 \approx 0.0005$ .

precisely at the Dirac point, then the conductivity dependence on the Fermi energy is linear and symmetric. However, we have demonstrated that the conductivity minimum is attained at the impurity resonance energy, which is essentially different from the Dirac point energy. This very difference does form the ground for the substantial conductivity asymmetry.

## VI. CONCLUSION

It is demonstrated that there are two scattering regimes, which characterize the behavior of the conductivity in graphene with point defects. In the weak scattering regime, i.e. when the impurity perturbation strength is less than the bandwidth, the dependence of the conductivity on the Fermi energy is monotonic and asymmetric, which can contribute to the observed conductivity asymmetry, when point defects does not dominate other sources of scattering. However, in the strong scattering regime, i.e. when the impurity potential exceeds the bandwidth, the conductivity caused by point defects manifests a distinctive minimum in its dependence on the Fermi energy. This minimum, in contrast to a majority

of anticipations, corresponds not to the Dirac point of the spectrum, but to the impurity resonance energy. In this regime, the asymmetry of the conductivity dependence on the Fermi energy is noticeable. What is more, the pronounced asymmetry of the corresponding dependence of the conductivity on the gate voltage is caused by the very shift of the conductivity minimum from the Dirac point to the impurity resonance energy. Despite the basic nature of the considered impurity model, it can qualitatively capture the essential features of the impure graphene conductivity manifested in experiments. Thus, one can expect that increasing the number of parameters characterizing the point defect will permit to approach closer to the quantitative description of conductivity features in graphene with point defects.

### Acknowledgments

Authors are grateful to V. P. Gusynin for valuable discussions. This work was supported by the SCOPES grant  $\mathcal{N}^\circ$  IZ73Z0-128026 of Swiss NSF, by the SIMTECH grant  $\mathcal{N}^\circ$  246937 of the European FP7 program, and by the Program of Fundamental Research of the Department of Physics and Astronomy of the National Academy of Sciences of Ukraine.

### Appendix: Diagonal element of Green's function

The straightforward expression for the diagonal element of the host Green's function reads:

$$g_{n\alpha n\alpha}(E) = \frac{1}{S_{BZ}} \int \frac{E}{E^2 - E^2(\mathbf{k})} d\mathbf{k}, \quad (\text{A.1})$$

where the integration is carried over the entire Brillouin zone, which has the area

$$S_{BZ} = \frac{8\pi^2}{\sqrt{3}a^2}, \quad (\text{A.2})$$

and  $E(\mathbf{k})$  is the unperturbed dispersion relation corresponding to the host Hamiltonian (1).

In practical situations the Fermi level in graphene is located, nearly unavoidably, in a narrow spectral region, in which the dispersion is linear with a good accuracy. Near each of the two inequivalent Dirac points, the dispersion relation  $E(\mathbf{k})$  can be expanded,

$$E(\mathbf{k}') \approx \pm v_F k', \quad (\text{A.3})$$

where  $\mathbf{k}'$  is taken relative to the corresponding Dirac point, and

$$v_F = \frac{\sqrt{3}at}{2}, \quad (\text{A.4})$$

is the Fermi velocity. Consequently, the integration in Eq. (A.1) over the wave vector can be also performed relative to the each Dirac cone vertex,

$$g_0(E) \approx \frac{2}{S_{BZ}} \int \frac{E}{E^2 - E^2(\mathbf{k})} d\mathbf{k}, \quad E \ll 3t, \quad (\text{A.5})$$

where the factor of 2 reflects the existence of two Dirac cones in the spectrum. However, due to the mutual overlap between respective cones, the integration in (A.5) can not be done over the entire Brillouin zone within the linear approximation for the dispersion relation. The corresponding cutoff magnitude of the wave vector is determined by the sum rule,

$$\frac{4\pi}{S_{BZ}} \int_0^{k_{max}} dk = 1, \quad (\text{A.6})$$

which yields

$$k_{max} = \frac{2\sqrt{\pi}}{\sqrt{\sqrt{3}a}}. \quad (\text{A.7})$$

Then, the integration can be performed exactly,

$$\begin{aligned} g_0(E) &\approx \frac{4\pi}{S_{BZ}} \int_0^{k_{max}} \frac{E}{E^2 - (v_F k)^2} k dk = \int_0^1 \frac{E}{E^2 - \sqrt{3}\pi t^2 x} dx = \\ &= \frac{\epsilon}{W} \left[ \ln \left( \frac{\epsilon^2}{1 - \epsilon^2} \right) - i\pi \operatorname{sgn} \epsilon \right], \quad E < W, \quad (\text{A.8}) \end{aligned}$$

where

$$W = \sqrt{\pi\sqrt{3}t}, \quad (\text{A.9})$$

is the bandwidth parameter for the pure Dirac spectrum.

<sup>1</sup> K. S. Novoselov, A. K. Geim, S. V. Morozov, D. Jiang, Y. Zhang, S. V. Dubonos, I. V. Grigorieva, and A. A. Firsov, *Science* **306**, 666 (2004).

<sup>2</sup> K. S. Novoselov, A. K. Geim, S. V. Morozov, D. Jiang, M. I. Katsnelson, I. V. Grigorieva, S. V. Dubonos, and A. A. Firsov, *Nature* **438**, 197 (2005).

<sup>3</sup> Y. Zhang, Y.-W. Tan, H. L. Stormer, and P. Kim, *Nature* **438**, 201 (2005).

<sup>4</sup> Y.-W. Tan, Y. Zhang, K. Bolotin, Y. Zhao, S. Adam, E. H. Hwang, S. Das Sarma, H. L. Stormer, and P. Kim, *Phys. Rev. Lett.* **99**, 246803 (2007).

<sup>5</sup> K. Nomura, and A. H. MacDonald, *Phys. Rev. Lett.* **98**, 076602 (2007).

<sup>6</sup> E. H. Hwang, S. Adam, and S. Das Sarma, *Phys. Rev. Lett.* **98**, 186806 (2007).

- <sup>7</sup> V. M. Galitski, S. Adam, and S. Das Sarma, *Phys. Rev. B* **76**, 245405 (2007) .
- <sup>8</sup> S. Adam, E. H. Hwang, E. Rossi, and S. Das Sarma, *Solid State Commun.* **149**, 1072 (2009).
- <sup>9</sup> J.-H. Chen, C. Jang, S. Adam, M. S. Fuhrer, E. D. Williams, and M. Ishigami, *Nature Phys.* **4**, 377 (2008).
- <sup>10</sup> J.-H. Chen, C. Jang, M. Ishigami, S. Xiao, W. G. Cullen, E. D. Williams, and M. S. Fuhrer, *Solid State Commun.* **149**, 1080 (2009).
- <sup>11</sup> L. A. Ponomarenko, R. Yang, T. M. Mohiuddin, M. I. Katsnelson, K. S. Novoselov, S. V. Morozov, A. A. Zhukov, F. Schedin, E. W. Hill, and A. K. Geim, *Phys. Rev. Lett.* **102**, 206603 (2009).
- <sup>12</sup> D. S. Novikov, *Appl. Phys. Lett.* **91**, 102102 (2007).
- <sup>13</sup> K. Pi, K. M. McCreary, W. Bao, Wei Han, Y. F. Chiang, Yan Li, S.-W. Tsai, C. N. Lau, and R. K. Kawakami, *Phys. Rev. B* **80**, 075406 (2009).
- <sup>14</sup> C. Jang, S. Adam, J.-H. Chen, E. D. Williams, S. Das Sarma, and M. S. Fuhrer, *Phys. Rev. Lett.* **101**, 146805 (2008).
- <sup>15</sup> A. Bostwick, J. L. McChesney, K. V. Emtsev, T. Seyller, K. Horn, S. D. Kevan, and E. Rotenberg, *Phys. Rev. Lett.* **103**, 056404 (2009).
- <sup>16</sup> Jian-Hao Chen, W. G. Cullen, C. Jang, M. S. Fuhrer, and E. D. Williams, *Phys. Rev. Lett.* **102**, 236805 (2009).
- <sup>17</sup> Yu. V. Skrypnik, and V. M. Loktev, *Phys. Rev. B* **73**, 241402(R) (2006).
- <sup>18</sup> S. Reich, J. Maultzsch, C. Thomsen, and P. Ordejón, *Phys. Rev. B* **66**, 035412 (2002).
- <sup>19</sup> R. W. Davies, and J. S. Langer, *Phys. Rev.* **131**, 163 (1963).
- <sup>20</sup> S. S. Pershoguba, Yu. V. Skrypnik, and V. M. Loktev, *Phys. Rev. B* **80**, 214201 (2009).
- <sup>21</sup> Hideki Kumazaki, and Dai S. Hirashima, *J. Phys. Soc. Jpn.* **75**, 053707 (2006).
- <sup>22</sup> A. F. Ioffe, and A. R. Regel, *Prog. Semicond.* **4**, 237 (1960).
- <sup>23</sup> Yuriy Skrypnik, *Phys. Rev. B* **70**, 212201 (2004).
- <sup>24</sup> Yu. V. Skrypnik, and V. M. Loktev, *Low Temp. Phys.* **33**, 762 (2007).
- <sup>25</sup> T. Stauber, N. M. R. Peres, and F. Guinea, *Phys. Rev. B* **76**, 205423 (2007).
- <sup>26</sup> Shaffique Adam, E. H. Hwang, V. M. Galitski, and S. Das Sarma, *Proc. Natl. Acad. Sci. USA* **104**, 18392 (2007).
- <sup>27</sup> T. Stauber, N. M. R. Peres, and A. H. Castro Neto, *Phys. Rev. B* **78**, 085418 (2008).